ADVANCED FUNCTIONAL MATERIALS
www.afm-journal.de

Effective Controlling of Film Texture and Carrier Transport of a High-Performance Polymeric Semiconductor by Magnetic Alignment

*Guoxing Pan, Fei Chen, Lin Hu, Kejun Zhang, Jianming Dai, and Fapei Zhang**

The controlling of molecular orientation and structural ordering of organic semiconductors is crucial to achieve high performance electronic devices. In this work, large-area highly oriented and ordered films of an excellent electron transporter Poly{[*N*,*N*′-bis(2-octyldodecyl)-1,4,5,8-naphthalenedicarboximide)-2,6-diyl]-alt-5,5′-(2,2′-bithiophene)} (P(NDI2OD-T2)) are achieved by improved solution-cast in high magnetic field. Microstructural characterizations reveal that the chain backbones of P(NDI2OD-T2) are highly aligned along the applied magnetic field in the films. Based on the synchrotron-based X-ray diffraction analysis of the polymer films cast from different solvents, a mechanism which controls the alignment process is proposed, which emphasizes that molecular aggregates of P(NDI2OD-T2) preformed in the solution initiate magnetic alignment and finally determine the degree of film texture. Furthermore, the time-modulated magnetic field technique is utilized to effectively control the orientation of π-conjugated plane of the backbones, thus the degree of face-on molecular packing of P(NDI2OD-T2) is enhanced significantly. Thin film transistors based on the magnetic-aligned P(NDI2OD-T2) films exhibit an enhancement of electron mobility by a factor of four compared to the unaligned devices, as well as a large mobility anisotropy of seven.

1. Introduction

Controlling film structure and nanomorphology of organic semiconductor, especially molecular packing and orientation, is crucial to achieve high performance of organic electronic devices. The "desired" molecular orientation depends on the device platforms. For example, the "face-on" packing in which the π-conjugated planes of the molecules are aligned with the substrates is conducive to charge transport in the stacked devices, e.g., solar cells.[1] However the "edge-on" orientation, in which the aromatic ring planes are aligned normal to the substrate, should be more favorable to lateral carrier transport in organic field-effect transistors (OFETs).[2] The control over molecular structure and processing conditions of thin films has been utilized to manipulate molecular orientation and ordering in the organic films.[1–3] On the other hand, macroscopically aligned film structure (so-called texture) is favorable to enhance carrier transport and to provide some unusual properties such as optically and electrically anisotropic characteristics.[4]

Over the past decades, a lot of deposition techniques have been developed to align organic semiconductors, for example the friction transfer[5] and nanoimprinting[6] for the polymers, the film deposition on the rubbed alignment layers,[7] as well as the solution processes such as zone casting,[8] solution shearing,[9] and the pinned drop casting on the inclined substrates.[10] Solution processed alignment provides a facile and effective approach to achieve the large area and highly ordered crystalline domains which enables a high carrier mobility. For example, an exceedingly high value of 8.1 and 43 $cm^2 V^{-1} s^{-1}$ was achieved in the OFETs of the highly oriented crystalline TIPS-pentacene[9b] and 2,7-dioctyl[1]benzothieno[3,2-b][1] benzothiophene films,[11] respectively. However, the alignment methods developed so far are usually molecule- and material-specific and many of them do not enable the orientation control in a simple and scalable way. Therefore, it will be of much significance to develop the effective and generalized strategies to control the ordering and alignment of organic semiconductors over large areas.

The attention was paid to utilize the external fields such as electric field or magnetic field to induce the molecular orientation on macroscopic length scale. Magnetic alignment originates from the anisotropy in diamagnetic susceptibility (χ) of organic molecules, which results in the anisotropy in free energy of molecule in magnetic field.[12] The magnetic approach provides a straightforward and clean (noncontact) method to fabricate large-area-oriented organic materials. Magnetic alignment at high field has been investigated widely on the molecular or polymeric liquid crystals (LCs)[13,14] as well as the block copolymers.[15,16] Furthermore, magnetically induced alignment for some kinds of crystalline nonconjugated

G. Pan, F. Chen, Dr. L. Hu, Prof. F. Zhang
High Magnetic Field Laboratory (HMFL)
Chinese Academy of Science
Hefei 230031, P. R. China
E-mail: fzhang@hmfl.ac.cn
G. Pan, Dr. L. Hu, Prof. F. Zhang
University of Science and Technology of China
Hefei 230026, P. R. China
K. Zhang, Prof. J. Dai
Key Laboratory of Materials Physics
Institute of Solid State Physics
Chinese Academy of Science
Hefei 230031, P. R. China

DOI: 10.1002/adfm.201500643

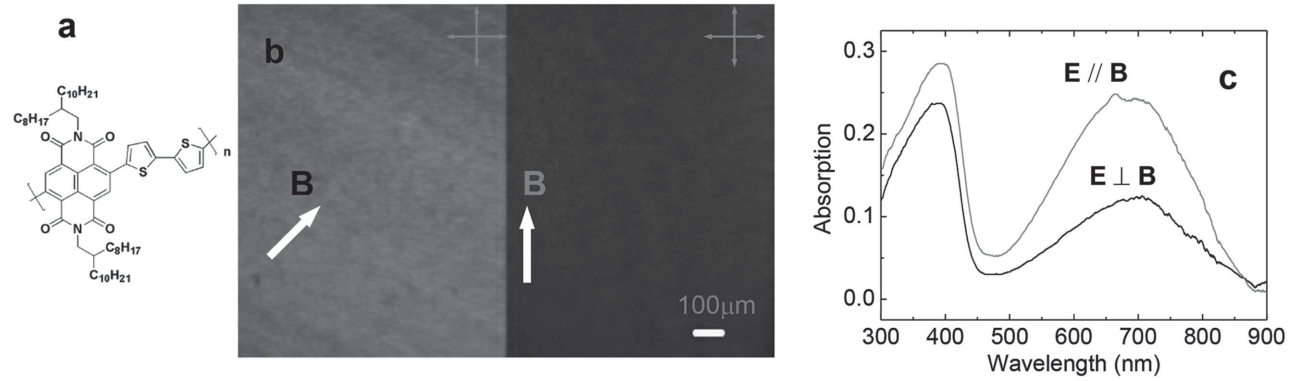

Figure 1. a) Chemical structure of P(NDI2OD-T2). b) POM images of a highly oriented P(NDI2OD-T2) film cast on the SiO_2/Si substrate from the DCB solution (0.5% w/w) under a magnetic field of 6 T. The white and red arrows indicate the magnetic field direction and the orientation of crossed polarizers, respectively. c) Polarized UV–vis absorption spectra of an aligned P(NDI2OD-T2) film on quartz. The direction of magnetic field applied during the growth is parallel (**B**//**E**) and perpendicular (**B**⊥**E**) to the polarization of the incident light, respectively.

polymers (e.g., poly(ethylene terephthalate)) was conducted from the melt crystallization process.[12,17] However, the materials studied so far mostly exhibit only low structural order and relatively weak intermolecular interaction. For the highly crystalline molecular semiconductors or semicrystalline polymers with strong π-stacking interaction, which exhibit high carrier mobility or good optoelectronic properties, the successful examples on structural manipulation by high magnetic field (HMF) were extremely scarce to date despite that highly oriented domain structure of the discotic LC hexabenzocoronene semiconductor (HBC-PhC12) was achieved via HMF.[13a] It is especially huge challenge for the fabrication of the oriented organic film by magnetic alignment, due to strong effect of the molecule-substrate interaction in this case.[18]

In this work, we demonstrate an example of high performance polymeric semiconductors in which effective structural manipulation of the polymer films is made by magnetic alignment. Recently low bandgap donor–acceptor (D–A) polymers,[19–21] consisting of alternate electron-rich and electron-poor units, were widely exploited in ambipolar OFETs and very efficient solar cells. The heterogeneity of the backbones with different D(A) units provides much complexity of interchain interaction, impacting deeply the way of chain assembly and packing, and consequently electronic properties in the films. Poly{[*N*,*N*′-bis(2-octyldodecyl)-1,4,5,8-naphthalenedicarboximide)-2,6-diyl]-alt-5,5′-(2,2′-bithiophene)} P(NDI2OD-T2) (see **Figure 1**a) is one of important D–A copolymers of excellent charge transport properties. It is an air-stable n-type transporter, exhibiting electron mobility as high as 0.85 $cm^2\ V^{-1}\ s^{-1}$ on the top-gated OFETs.[22] Despite nonpronounced long-range ordering as many other D–A polymers, the films of P(NDI2OD-T2) exhibit predominantly face-on packing and a high degree of in-plane nanoorganization.[23,24] Notably, molecular packing can be switched from face-on to edge-on motif by annealing the as-cast film above 300 °C.[25] The control over the in-plane molecular orientation and stacking has also been performed via epitaxial crystallization on trichlorobenzene or epitaxy on the aligned substrates.[26] Chain backbones of P(NDI2OD-T2) possess large-size π-conjugated plane and a strong interchain π–π stacking, which is expected to exhibit a large anisotropy of χ as well as strong interaction between magnetic field and chain backbones. Here, we report that molecular orientation and film texture can be effectively controlled during film growth by solution cast at high magnetic field, and also found such structural tuning plays a crucial role on carrier transport of the P(NDI2OD-T2) devices. To the best of our knowledge, it is the first report on the achievement of magnetic manipulation of film structure for semicrystalline (or crystalline) polymer semiconductors with good carrier transport.

2. Results and Discussion

2.1. In-Plane Structure of Magnetically Aligned P(NDI2OD-T2) Films

Highly aligned films were deposited on the Si/SiO_2 substrates by drop casting from the 0.1%–0.8% P(NDI2OD-T2) solution in a horizontal superconducting magnet at room temperature. The growth rate was controlled by slow solvent evaporation (see the Experimental Section). Polarized optical microscopy (POM) images of the P(NDI2OD-T2) films exhibit a homogeneous change of brightness as shown in Figure 1b. The brightness of the POM image was maximized when the angle between the applied field and the polarizer was ±45° while minimized when such an angle was 90°(or 0°), indicating a large-area texture structure covered on the entire substrate. We found that the highly oriented "monodomain" in centimeter size can be obtained at the magnetic field of higher than 6 T. The similar results are also observed for the film fabrication of other semiconducting polymers for example poly(2,5-bis(2-alkylthiophene-2-yl)thieno[3,2-b]thiophene (PBTTT) (see Figure S1, Supporting Information). As a comparison, the films drop cast via the same procedures however without the applied field, exhibit an isotropic (unaligned) character as shown in Figure S2 (Supporting Information).

The aligned film structure is also evidenced by the polarized UV–vis spectra of the P(NDI2OD-2T) films, which shows clear absorption anisotropy with a dichroic ratio of 2:3 (in Figure 1c). Stronger absorption takes place on the broad band centered at 700 nm and with a vibronic shoulder at 810 nm, when the direction of magnetic field applied during film cast

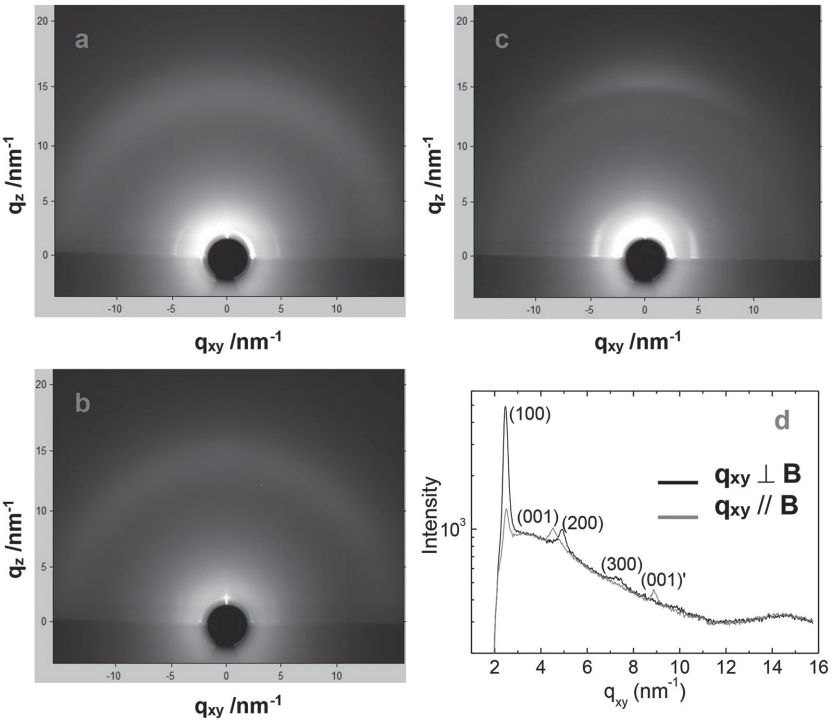

Figure 2. a,b) 2D GIXRD patterns of the magnetically aligned P(NDI2OD-T2) film cast from the DCB solution (0.2% w/w) under a field of 8 T, with in-plane scattering vector q_{xy} nominally perpendicular and parallel to the magnetic field direction, respectively. c) The GIXRD pattern of a solution-cast, isotropic film. d) Cross-section profiles of the 2D diffraction patterns along the q_{xy} direction shown in (a) and (b).

is parallel to polarization direction of the incident light. Since the dipole moment of the main electronic transition is oriented along the polymer backbone, it indicates that the chain backbones of P(NDI2OD-2T) should be aligned preferentially with the field direction. Interestingly, in spite of the large absorption dichroism at low energy region, the magnetically aligned P(NDI2OD-2T) is characteristic of a weakly polarized high-energy absorption band at 393 nm. The high- and low-energy absorption band was assigned to π–π^* excitation and intrachain charge transfer excitation, respectively. Such an absorption behavior is very similar to that for the highly aligned P(NDI2OD-2T) films deposited via directional epitaxial crystallization, which was assigned to the presence of segregated stacks of nanphthalene dimide (NDI) and bithiophene (T2) units in P(NDI2OD-2T) film.[26]

To give deeper insight into the effect of magnetic alignment on the molecular orientation and crystalline domains of the P(NDI2OD-2T) films, synchrotron-based grazing incidence X-ray diffraction (GIXRD) were performed as shown in **Figure 2**. A 2D GIXRD pattern of the isotropic film as-cast (Figure 2c), reveals a weak (010) reflection along out-of-plane direction (nominally q_z), as well as the mixed two families of the reflections at the in-plane direction ($q_z \approx 0$). However, when the X-ray beam is parallel and perpendicular to magnetic alignment (that is, in-plane scatter vector q_{xy} is nearly perpendicular and parallel to the field direction), respectively, the GIXRD patterns of the aligned films show large difference in the diffraction positions and intensity (Figure 2a,b), which is manifested clearly in the cross-section profiles along q_{xy} (Figure 2d). When the q_{xy} is perpendicular to the magnetic field, the diffraction pattern reveals the (h00) series reflections, assigned to lamellar stacking (d-spacing d_{100} is 2.57 nm).[25] However, when the scatter vector is parallel to the field, two peaks appear at the q_{xy} of 0.45 and 0.88 nm^{-1}, which are assigned to (001) and (001)' reflection, respectively, related to chain backbone repeat.[25] The strong anisotropy of in-plane ordering reflects the local spatial arrangement of polymer chains. It clearly confirms that chain backbones of P(NDIOD-T2) are highly aligned with the magnetic field and lie on the substrate within the crystallites in the deposited film, which finally results in macroscopic texture structure. The degree of in-plane alignment is found to increases with magnitude of the field. On the other hand, the π-stacking (010) reflection becomes slightly broader and weaker compared to the isotropic films. It is consistent with a considerably broad out-of-plane intensity distribution of the (h00) peaks in Figure 2a,b, indicating a less in-plane orientation of lamellar stacking. However, the face-on molecular packing is still preserved largely for the magnetically aligned films.

2.2. Origin for Magnetic Alignment of P(NDIOD-T2)

In order to explain above observations, the origin of magnetic alignment of P(NDIOD-T2) should be elucidated in more detail. In the previous investigations on magnetic alignment of the LC polymers,[14] nematic nuclei were found to form during cooling from the isotropic melt into the LC phase. The existence of residual tiny ordered structures (referred as mesophase) was also proposed for the melts of crystalline polymers such as PEN and PET.[12,17a] Sufficiently large ordered nuclei (and thus with large anisotropy of magnetic energy) can be aligned by magnetic field and consequently initiate the formation of macroscopic orientation domains. In the present case, we suggest that some kinds of tiny molecular assembles of P(NDI2OD-T2) also exist in the solution, acting as the directors for magnetic alignment during film deposition. Recently Steyrleuthner et al., found that the chains of P(NDI2OD-T2) take aggregation (the stacking of polymer chains) in the solutions of various solvents and the aggregate content strongly depends on the type of solvents.[27,28] We prepared the P(NDI2OD-T2) solutions using three kinds of common solvents (DCB was utilized in above experiments), among which the chlorobenzene (CB) solution exhibits the highest degree of aggregation and no aggregation takes place in the chloronaphthalene (CN).[27] Varied degree of preaggregation in the solution was made to investigate its role on the magnetically induced growth behavior of P(NDI2OD-T2).

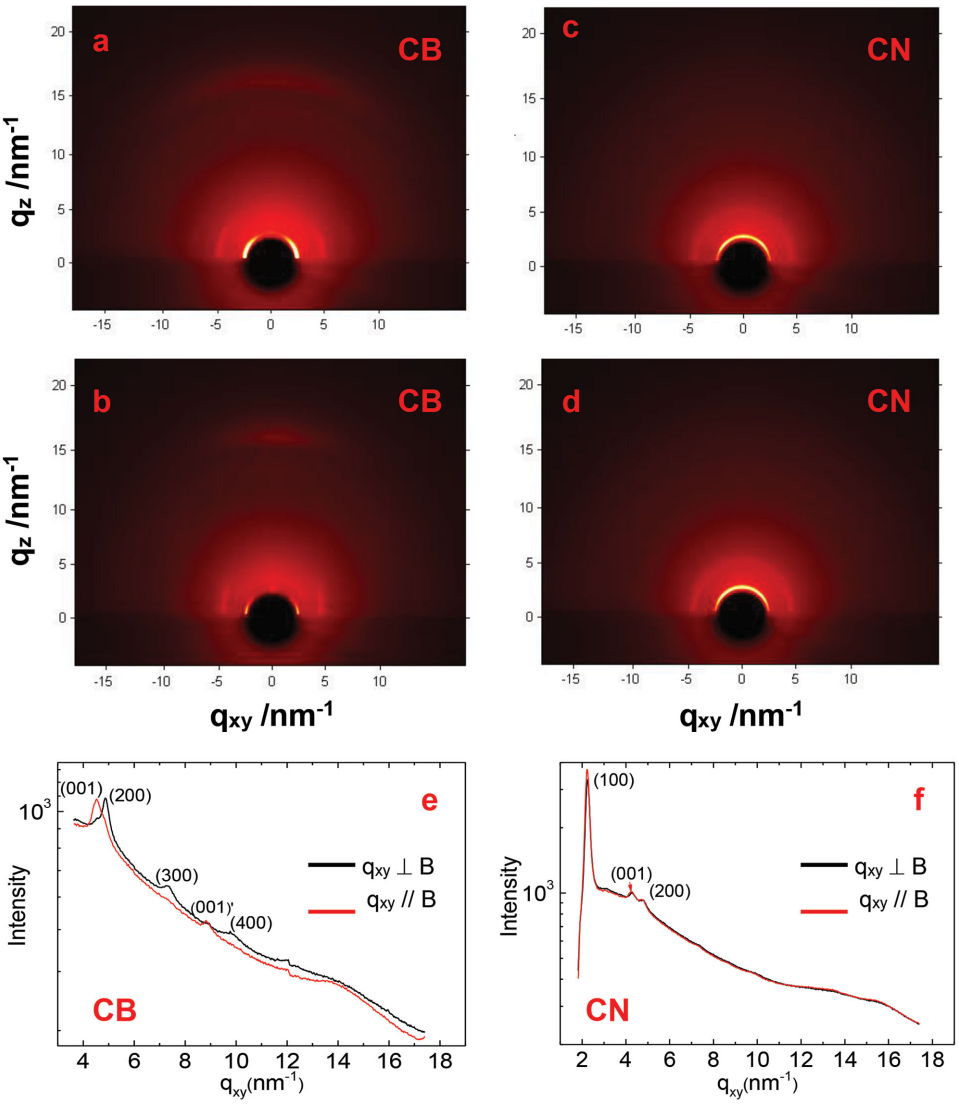

Figure 3. Comparison of 2D GIXRD patterns of the aligned P(NDI2OD-T2) films cast from 0.2% solution of a,b) CB and of c,d) CN, respectively. The q_{xy} is nominally a–c) perpendicular and b–d) parallel to the field direction, respectively. e,f) Cross-section profiles of the 2D diffraction patterns shown in Figure a,b and Figure c,d along the q_{xy} direction.

Figure 3 shows the 2D GIXRD patterns of the P(NDI2OD-T2) films drop cast from the CB and CN solution in high magnetic field, respectively. In spite of the same chain alignment with external field, the film cast from CB shows the stronger diffraction intensities in both the q_z- and q_{xy}-directions (Figure 3a,b) compared with the samples from the DCB solution. The high orders of in-plane (h00) reflections up to fourth are observed in Figure 3e, which manifests higher degree of structural ordering and alignment, probably related to the larger size and more volume fraction of the aligned crystallinites within the film. On the other hand, no difference can be found on the in-plane diffraction patterns for the films cast from CN no matter whether the scatter vector q_{xy} is parallel or perpendicular to the magnetic field (in Figure 3c,d), indicating no preferential alignment of the polymer chains. Therefore, the higher aggregate contents in the solution correspond to the higher degree of structural ordering and film texture. It will be noted that the face-on chain packing, exhibited on the P(NDI2OD-T2) films grown from DCB or CB, is switched predominantly into the edge-on packing for the films cast from CN, in consistent with the observation reported by Steyrleuthner et al.[28]

Based on above results, we propose that the preaggregation of P(NDI2OD-T2) in the solution plays a critical role on determining the magnetic alignment behavior of the cast films. Surprisingly, it was found that the aggregation of conjugated segments takes place via stacking within polymer coils that contain one or few chains of P(NDI2OD-T2).[27] However, the large-size conjugated plane of the repeat units (NDI and T2), together with high molecular weight (M_W) of the polymer, will warrant the aggregates of P(NDI2OD-T2) a large volume (V_a) and thus sufficiently high anisotropy of magnetic energy ($V_a\Delta\chi B^2/2\mu_o \gg$ thermal energy k_BT, $\Delta\chi$: the difference in χ between two axes parallel and perpendicular to chain backbone). Such free energy gain enables the rotation and consequently the alignment of

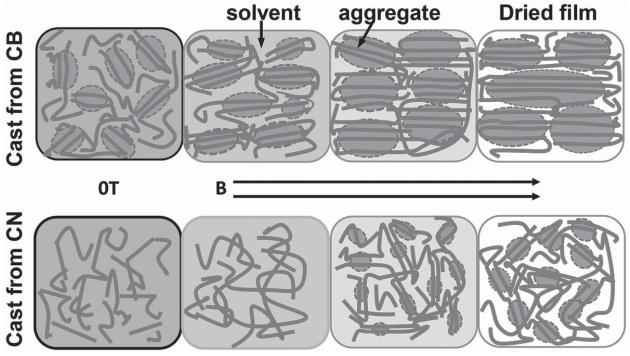

Figure 4. Schematic illustration of the magnetic alignment process in the formation of the P(NDI2OD-T2) film cast from CB (top) and CN (bottom) under high magnetic field. The thick lines denote the chains of P(NDI2OD-T2).

molecular aggregates in low viscosity environment (solvent) at external magnetic field. The magnetic-induced growth process of the P(NDI2OD-T2) film is described schematically in the **Figure 4**. For solution cast from the aggregate-containing solvent (top of Figure 4), the oriented aggregates (ordered "nuclei") can act as the director for the alignment of more P(NDI2OD-T2) chains. Some of the aligned aggregates merge into the larger size-oriented domains with solvent evaporation, which finally lead to the formation of macroscopically aligned film. Such proposed growth dynamics shows much similarity with magnetic alignment of the crystalline polymer PET during cooling from the melts.[17a] Furthermore, higher degree of molecular aggregates inhibits the formation of the amorphous films and facilitates the growth of large-size ordered grains in the films. In the case of no aggregation (bottom of Figure 4), individual polymer coils with swollen chain conformation in the CN solution could not get rise to large enough anisotropy of magnetic energy (smaller than k_BT) to trigger magnetic alignment.

The aggregate-triggered magnetic alignment will be of much significance to solution processing of the semiconducting polymers. Many kinds of recently developed D–A polymers exhibit clear signature of molecular aggregation in the solution due to strong interchain interaction and propensity to self-assemble.[19b,20,29] Magnetic approach based on above strategy will provide an effective route to manipulate film microstructures of these materials and thus to control over charge transport, exciton diffusion, and charge separation processes in the OFETs and solar cells.

2.3. Magnetic Manipulation of Out-of-Plane Molecular Orientation of P(NDIOD-T2) Films

In addition to the control over in-plane film texture, the effort on the manipulation of the out-of-plane molecular orientation was also performed by HMF. A large field of 9 T was applied perpendicular to the substrate surface during solution-cast of P(NDI2OD-T2). The specular scan X-ray diffraction pattern in Figure S3a (Supporting Information) shows that the (010) reflection from the cast film, assigned to the interchain face-on packing, is drastically weakened with respect to the samples cast without the magnetic field. It is not unexpected because the face-on packing is not energetically favorable at the field perpendicular to the substrate, because absolute value of diamagnetic susceptibility $|\chi|$ of P(NDI2OD-T2) is maximized when the field direction is normal to the conjugated planes of polymer backbones. However, the (100) reflection assigned to the edge-on packing order is also suppressed slightly, although such packing motif is assumed to be energetically favorable in this situation. It may be attributed to structural disorder introduced by magnetic manipulation. It should be pointed out that, out-of-plane molecular orientation and film texture show no any difference among the P(NDI2OD-T2) films cast from CN solution, no matter whether the perpendicular magnetic field is applied (see Figure S3b, Supporting Information).

As shown from previous sections, the "uniaxial" magnetic alignment processing does not improve (even reduce) the degree of the face-on packing of P(NDI2OD-T2) backbones. It should be attributed to the degeneracy on spatial orientation of the interchain π-stacking with respective to substrate surface, as shown in Figure S4b (Supporting Information). Under such circumstance, although the chain backbones tend to align with their conjugated ring planes parallel to the magnetic field, the direction of interchain π-stacking in the mesophases (crystallites) may lie at any angle in the plane perpendicular to the field (i.e., magnetic isoenergetic irrespective of face-on or edge-on motif). In order to make a better control over out-of-plane molecular packing, we applied the technique based on the continuous rotation of the substrate on an axis perpendicular to the magnetic field during solution cast[30] shown schematically in **Figure 5**a. This processing could break the degeneration on spatial arrangement of chain backbones, and enables the "flat-lying" packing motif of conjugated planes of P(NDI2OD-T2) in the mesopahse a minimum of average magnetic energy. Specular XRD patterns in Figure 5b exhibit an intensity enhancement of the (010) reflection by a factor of 2.5 while a decreased intensity of the (100) peak for the P(NDI2OD-T2) film cast via rotating the substrate (5 rpm) in a magnetic field of 8 T, compared to the isotropic films. It indicates a remarkable enhancement on the degree of face-on packing, which is correlated to increased fraction of the platelet-like crystallites with interchain π-stacking direction aligned to substrate normal in the film, as shown in Figure S4c (Supporting Information). Interestingly, a

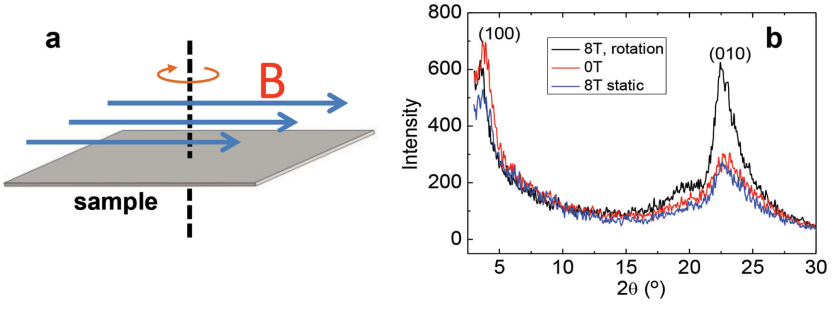

Figure 5. a) Geometry of magnetic alignment experiment with the sample rotating in the magnetic field. b) Specular scan diffraction patterns of the P(NDI2OD-T2) films cast in absent of magnetic field (red line), under a 8 T field w/o the sample rotating (blue line) as well as under a 8 T field with the geometry shown in (a) (black line).

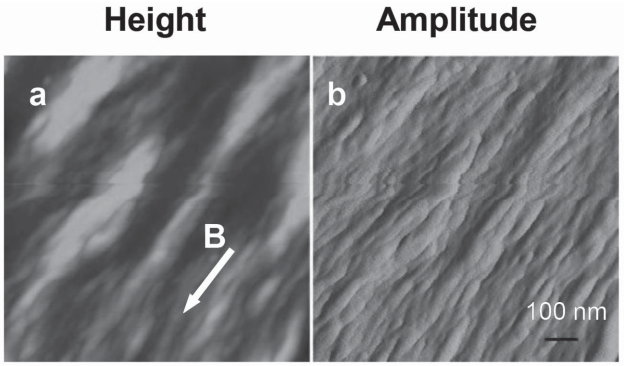

Figure 6. a) AFM height and b) amplitude images of a P(NDI2OD-T2) film cast from 0.2% CB solution under a magnetic field of 8 T. The magnetic field direction is indicated by an arrow.

large extent of in-plane texture can still be achieved on the films cast via rotating the samples in magnetic field and sequentially holding the substrate statically under the same field before the wet film is dried (not shown here). The effective manipulation on the degree of out-of-plane molecular orientation is commonly difficult for the π-conjugated polymers. The method proposed here would present a nice pathway to optimize out-of-plane film microstructures and thus improve carrier transport in the sandwich-type devices e.g., solar cells and diodes. The relevant effects on electrical properties are under the investigation.

2.4. Morphology of Magnetically Aligned Films

Surface morphology of the films is crucial to achieve high-quality organic devices. **Figure 6** shows the tapping-mode atomic force microscopy (AFM) images for the magnetically aligned P(NDI2OD-T2) films cast from CB. The aligned films cast from both the CB and the DCB solutions (in Figure S5, Supporting Information), exhibit a highly oriented nanofibril-like structure, which are aligned parallel to the direction of magnetic field. Since the polymer backbones are found to orient along the field direction, the fibrillar structures should be composed of the in-plane aligned chains of P(NDI2OD-T2). However, the nanofibrils shown on the CB-cast films possess the larger length (ca. 100–400 nm) and higher orientation order, indicating the more ordered crystallites within the film. It verifies that the higher degree of the preaggregation leads to the higher film texture and ordering by magnetic alignment as indicated in the GIXRD results. In addition, these nanofibrils have a width of 20–30 nm. The order in width direction originates from lamellar stacking of the side chains of P(NDI2OD-T2). Such width scale is comparable to the coherence length (width of crystallite platelet) estimated from the full width at half maximum of the (100) peak Δ_{100} (0.2 nm^{-1}) in Figures 2 and 3 based on Scherrer equation.

2.5. Carrier Transport Studies

To directly assess the impact of magnetic alignment on charge transport properties, bottom-contact/bottom-gated TFTs were fabricated based on the P(NDI2OD-T2) films cast at high magnetic field. They were compared with the nonaligned devices which took the same fabrication procedures after film casting. **Figure 7**a shows typical transfer curves for the devices of the aligned films cast from CB solution, with current direction parallel and perpendicular to applied magnetic field, respectively (output curves of the "parallel" devices are shown in Figure S6, Supporting Information). All of the devices exhibit good n-type operation behavior with a high on/off ratio of 10^5 and good operating stability. Notably, the TFTs with current direction parallel to the magnetic field (the "parallel devices"), exhibit a significantly larger drain current I_D than the devices with the channel perpendicular to the field direction, as well as the isotropic devices (in Figure S7, Supporting Information). Reasonably high electron mobility of 0.092 cm^2 V^{-1} s^{-1} is extracted in saturation region for the parallel device, which is enhanced by a factor of four with respect to isotropic devices. The anisotropy of electron mobility ($\mu_{||}/\mu_{\perp,}\mu_{||(\perp)}$: mobility parallel (perpendicular) to the magnetic field) is ca. 7. This unequivocally demonstrates that molecular orientation and film texture induced by magnetic alignment crucially influences charge transport of the high performance polymer P(NDI2OD-T2).

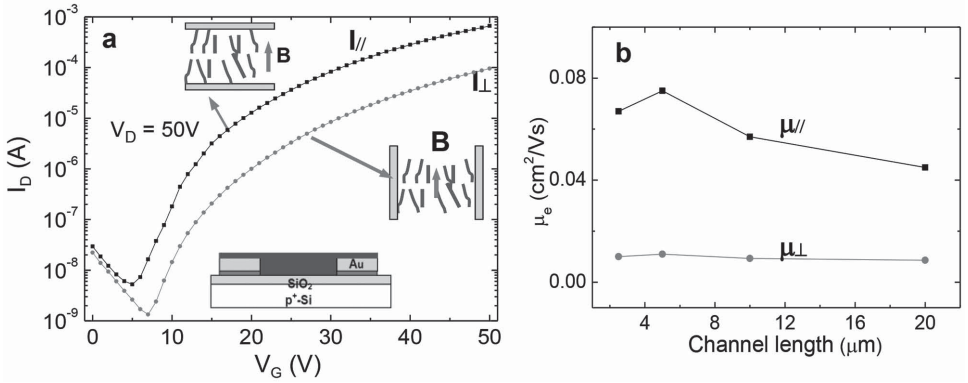

Figure 7. Electrical performance of the magnetically aligned P(NDI2OD-T2) based TFTs. a) Typical transfer characteristics for a TFT device (L = 5 μm and W = 10 mm) of the oriented film, with the channel current parallel ($I_{//}$, black line) and perpendicular ($I_{\perp}$, red line) to the magnetic field direction. The insets schematically show current direction with respect to the field direction B, as well as device geometry of a bottom-contact TFT. b) Dependence of electron mobility on channel length for both current directions: $\mu_{//}$ and $\mu_{\perp}$ is extracted from the V_G dependence of $I_{//}$ and $I_{\perp}$, respectively.

Higher $\mu_{||}$ is mainly attributed to fast intrachain charge transport along the polymer backbones in the ordered crystallites[31] which are aligned with the field direction. It will be pointed out that the TFTs based on the films cast from CN in magnetic field, exhibit no mobility anisotropy but a lowered mobility values than the isotropic devices.

Figure 7b shows the variation of electron mobility $\mu_{||(\perp)}$ as a function of channel length. Each of $\mu_{||\ (\perp)}$ values shown is averaged for four devices. The dependence of channel length is relatively weak especially for the $\mu_{\perp}$ values. It may be relevant to macroscopically homogenous morphology of the magnetic aligned P(NDI2OD-T2) films, as well as good electrical connection pathway at the boundaries of the ordered crystallites. The increase of $\mu_{||}$ with the decreased channel length is related to the reduced numbers of grain boundaries along current direction. The good device characteristics and favorable film morphology suggest that magnetic alignment processing is compatible to the common TFT fabrication. However, the output curves in Figures S6 and S7b (Supporting Information) show a clear super linear increase of I_D at low drain voltage V_D, indicating considerable large contact resistance on these devices.[32] The higher TFT performance will be expected if device fabrication conditions are improved further, e.g., via the treatments of substrate surface, the fine control over solvent evaporation during film cast, as well as the lowering of contact resistance by the modification of source/drain contacts by self-assembly monolayers (SAMs).

3. Conclusions

Molecular orientation and film texture of P(NDI2OD-T2) in both in-plane and out-of-plane direction have been controlled effectively via in situ solution casting of the polymer films at high magnetic field. Based on comprehensive structural characterizations such as AFM and X-ray diffraction, the mechanism on magnetically induced growth of P(NDI2OD-T2) was elucidated, which proposed that strong interaction between magnetic field and the aggregates of polymer chains directs the chain alignment and the formation of macroscopic orientation film structure. The magnetically aligned P(NDI2OD-T2) films display remarkably enhanced electron mobility and high mobility anisotropy. The successful manipulation of film microstructure and nanomorphology of P(NDI2OD-T2), a D–A type polymer exhibiting a strong interchain interaction and high structural order, demonstrates magnetic field as a promising approach to improve electrical and optical properties of high performance semiconducting polymers in the devices such as OFETs and organic solar cells.

4. Experimental Section

P(NDI2OD-T2) was purchased from Polyera Corporation (Activink N2200) and used as received. Alignment experiments were performed in a horizontal 9 T superconducting magnet (Cryomagnetics, Inc.) as well as a vertical 10 T superconducting magnet (AMI American Magnetics, Inc.). The aligned films were prepared by drop casting the P(NDI2OD-T2) solutions (0.1%–0.8% w/w) of different solvents on the flat Si/SiO_2 substrates under the magnetic field at room temperature. During solution cast, the sample was placed in the covered glass Petri dish to slow down solvent evaporation. For the film cast from CN, the substrate was heated at 45 °C during the cast and uncovered by Petri dish. The magnetic field was applied until the solvent was evaporated. The film thickness was in the range of 80–650 nm as measured by a surface profilometer.

For the characterization of magnetic alignment, 2D grazing incidence X-ray diffraction (GIXRD) measurement was performed at Shanghai Synchrotron Radiation Facility (SSRF) on the beam line BL14B with the photon energy of 10.0 keV (wavelength, $\lambda = 1.2398$ Å). A MAR CCD (3072 pixels) area detector was used to measure the 2D diffraction intensities. The incidence angle of X-ray beam is 0.2°. Specular scan X-ray diffraction experiment was performed on a Rigaku-TTR3 X-ray diffractometer with Cu $K\alpha$ ($\lambda = 1.5406$ Å) radiation. The morphology of the P(NDI2OD-T2) films was characterized with a Veeco MultiMode (Nanoscope V) AFM in tapping mode under ambient conditions. Optical anisotropy of the aligned films was probed by polarized light microscope as well as UV–vis absorption spectroscopy in transmission geometry with polarized incident light (on quartz substrates).

For the fabrication of the FET samples based on the aligned films, bottom-gate/bottom-contact devices were fabricated on heavily doped Si wafers with a 400 nm thermally grown SiO_2 layer. The surface of the Si/SiO_2 substrates were prepatterned with interdigitated electrode arrays of Au (30 nm) with a 10 nm ITO adhesive layer by photolithography, act as source/drain electrodes. The electrode arrays are characteristic of the channel width (W) of 10 mm and different channel length (L) from 2.5 to 20 μm. The wafers were cleaned through subsequent sonication with acetone and isopropanol and cleaned in a UV-ozone cleaner. The polymer films were drop cast in situ as described above. Finally, as-prepared films were annealed at 145 °C for 1 h in nitrogen atmosphere to remove remnant solvent. The electrical measurements were performed on a probe station by a two-channel source meter (Keithley 2612A) in the glove box. Field-effect mobility (μ_{FET}) was calculated in the saturation regime using the transistor equation

$$I_D = \frac{WC_i\mu_{FET}(V_G - V_T)^2}{2L}$$

where C_i (8.91 nF cm^{-2}) is the area capacitance of the SiO_2 dielectric and V_G and V_{th} is gate voltage and threshold voltage, respectively.

Supporting Information

Supporting Information is available from the Wiley Online Library or from the author.

Acknowledgements

This work was supported financially by the Chinese Academy of Sciences (CAS) and the National Natural Science Foundation of China (NSFC, Grant No. 11074256), as well as Scientific Research Grant of Hefei Science Center of CAS (SRG-HSC, Grant No. 2015SRG-HSC020). The authors thank J. Fang and L. Zhang at HMFL for assistance on the operation of the SC magnet and on the (specular scan) X-ray diffraction measurement. The technique assistance on the GIXRD experiment from the staffs in the BL14B station at Shanghai Synchrotron Radiation Facilities is also gratefully acknowledged.

Received: February 15, 2015
Revised: June 5, 2015
Published online: July 14, 2015

[1] A. M. Hiszpanski, Y. L. Loo, *Energy Environ. Sci.* **2014**, *7*, 592.
[2] H. Sirringhaus, P. J. Brown, R. H. Friend, M. M. Nielsen, K. Bechgaard, B. M. W. Langeveld-Voss, A. J. H. Spiering, R. A. J. Janssen, E. W. Meijer, P. Herwig, D. M. de Leeuw, *Nature* **1999**, *401*, 685.

[3] C. W. Sele, B. K. C. Kjellander, B. Niesen, M. J. Thornton, J. B. P. H. van der Putten, K. Myny, H. J. Wondergem, A. Moser, R. Resel, A. J. J. M. van Breemen, *Adv. Mater.* **2009**, *21*, 4926.
[4] S. Liu, W. M. Wang, A. L. Briseno, S. C. B. Mannsfeld, Z. Bao, *Adv. Mater.* **2009**, *21*, 1217.
[5] M. Misaki, Y. Ueda, S. Nagamatsu, Y. Yoshida, N. Tanigaki, K. Yase, *Macromolecules* **2004**, *37*, 6926.
[6] Z. Zheng, K. Yim, M. S. M. Saifullah, M. E. Welland, R. H. Friend, J. S. Kim, W. T. S. Huck, *Nano Lett.* **2007**, *7*, 987.
[7] a) H. Sirringhaus, R. J. Wilson, R. H. Friend, M. Inbasekaran, W. Wu, E. P. Woo, M. Grell, D. D. C. Bradley, *Appl. Phys. Lett.* **2000**, *77*, 406; b) A. J. J. M. van Breemen, P. T. Herwig, C. H. T. Chlon, J. Sweelssen, H. F. M. Schoo, S. Setayesh, W. M. Hardeman, C. A. Martin, D. M. de Leeuw, J. J. P. Valeton, C. W. M. Bastiaansen, D. J. Broer, A. R. Popa-Merticaru, S. C. J. Meskers, *J. Am. Chem. Soc.* **2006**, *128*, 2336.
[8] a) A. Tracz, J. K. Jeszka, M. D. Watson, W. Pisula, K. Muellen, *J. Am. Chem. Soc.* **2003**, *125*, 1682; b) W. Pisula, A. Menon, M. Stepputat, I. Lieberwirth, U. Kolb, A. Tracz, H. Sirringhaus, T. Pakula, K. Muellen, *Adv. Mater.* **2005**, *17*, 684.
[9] a) H. A. Becerril, M. E. Roberts, Z. Liu, J. Locklin, Z. Bao, *Adv. Mater.* **2008**, *20*, 2588; b) Y. Diao, B. C.-K. Tee, G. Giri, J. Xu, D. H. Kim, H. A. Becerril, R. M. Stoltenberg, T. H. Lee, S. C. B. Mannsfeld, Z. Bao, *Nat. Mater.* **2013**, *12*, 665.
[10] T. Uemura, Y. Hirose, M. Uno, K. Takimiya, J. Takeya, *Appl. Phys. Express* **2009**, *2*, 111501.
[11] Y. Yuan, G. Giri, A. L. Ayzner, A. P. Zoombelt, S. C. B. Mannsfeld, J. Chen, D. Nordlund, M. F. Toney, J. Huang, Z. Bao, *Nat. Commun.* **2014**, *5*, 3005.
[12] T. Kimura, *Polym. J.* **2003**, *35*, 823.
[13] a) I. O. Shklyarevskiy, P. Jonkheijm, N. Stutzmann, D. Wasserberg, H. J. Wondergem, P. C. M. Christianen, A. P. H. Schenning, D. M. de Leeuw, Z. Tomovic, J. Wu, K. Muellen, J. C. Maan, *J. Am. Chem. Soc.* **2005**, *127*, 16233; b) H. S. Kim, S.-M. Choi, J.-H. Lee, P. Busch, S. J. Koza, E. A. Verploegen, B. D. Pate, *Adv. Mater.* **2008**, *20*, 1105.
[14] a) M. I. Boamfa, K. Viertler, A. Wewerka, F. Stelzer, P. C. M. Christianen, J. C. Maan, *Phys. Rev. Lett.* **2003**, *90*, 025501; b) K. Akagi, *Bull. Chem. Soc. Jpn.* **2007**, *80*, 649.
[15] a) Y. Tao, H. Zohar, B. D. Olsen, R. A. Segalman, *Nano Lett.* **2007**, *7*, 2742; b) B. McCulloch, G. Portale, W. Bras, J. A. Pople, A. Hexemer, R. A. Segalman, *Macromolecules* **2013**, *46*, 4462.
[16] a) H. Tran, M. Gopinadhan, P. W. Majewski, R. Shade, V. Steffes, C. O. Osuji, L. M. Campos, *ACS Nano* **2013**, *7*, 5514; b) P. W. Majewski, M. Copinadhan, C. O. Osuji, *Polymer Phys.* **2012**, *50*, 2.
[17] a) T. Kimura, T. Kawai, Y. Sakamoto, *Polymer* **2000**, *41*, 809; b) N. Naga, G. Ishikawa, K. Noguchi, K. Takahashi, K. Watanabe, *Polymer* **2013**, *54*, 784.
[18] H. Yonemura, K. Yuno, Y. Yamamoto, S. Yamada, Y. Fujiwara, Y. Tanimoto, *Synth. Met.* **2009**, *159*, 955.
[19] a) C. B. Nelson, M. Turbiez, I. McCulloch, *Adv. Mater.* **2013**, *25*, 1859; b) X. Zhang, L. J. Richter, D. M. DeLongchamp, R. J. Kline, M. R. Hammond, I. McCulloch, M. Heeney, R. S. Ashraf, J. N. Smith, T. D. Anthopoulos, B. Schroeder, Y. H. Geerts, D. A. Fischer, M. F. Toney, *J. Am. Chem. Soc.* **2011**, *133*, 15073; c) H. Chen, Y. Guo, G. Yu, Y. Zhao, J. Zhang, D. Gao, H. Liu, Y. Liu, *Adv. Mater.* **2012**, *24*, 4618; d) H. N. Tsao, D. M. Cho, I. Park, M. R. Hansen, A. Mavrinskiy, D. Y. Yoon, R. Graf, W. Pisula, H. W. Spiess, K. Müllen, *J. Am. Chem. Soc.* **2011**, *133*, 2605.
[20] P. M. Beaujuge, J. M. J. Fréchet, *J. Am. Chem. Soc.* **2011**, *133*, 20009.
[21] X. Zhang, H. Bronstein, A. J. Kronemeijer, J. Smith, Y. Kim, R. J. Kline, L. J. Richter, T. D. Anthopoulos, H. Sirringhaus, K. Song, M. Heeney, W. Zhang, I. McCulloch, D. M. Delongchamp, *Nat. Commun.* **2013**, *4*, 2238.
[22] a) Z. Chen, Y. Zheng, H. Yan, A. Facchetti, *J. Am. Chem. Soc.* **2009**, *131*, 8; b) H. Yan, Z. Chen, Y. Zheng, C. Newman, J. R. Quinn, F. Dötz, M. Kastler, A. Facchetti, *Nature* **2009**, *457*, 679.
[23] J. Rivnay, M. F. Toney, Y. Zheng, I. V. Kauvar, Z. Chen, V. Wagner, A. Facchetti, A. Salleo, *Adv. Mater.* **2010**, *22*, 4359.
[24] T. Schuettfort, L. Thomsen, C. R. McNeill, *J. Am. Chem. Soc.* **2012**, *135*, 1092.
[25] J. Rivnay, R. Steyrleuthner, A. Jimison, A. Casadei, Z. Chen, M. F. Toney, A. Facchetti, D. Neher, A. Salleo, *Macromolecules* **2011**, *44*, 5246.
[26] M. Brinkmann, E. Gonthier, S. Bogen, K. Tremel, S. Ludwigs, M. Hufnagel, M. Sommer, *ACS Nano* **2012**, *6*, 10319.
[27] R. Steyrleuthner, M. Schubert, I. Howard, B. Klaumünzer, K. Schilling, Z. Chen, P. Saalfrank, F. Laquai, A. Facchetti, D. Neher, *J. Am. Chem. Soc.* **2012**, *134*, 18303.
[28] R. Steyrleuthner, R. D. Pietro, B. A. Collins, F. Polzer, S. Himmelberger, M. Schubert, Z. Chen, S. Zhang, A. Salleo, H. Ade, A. Facchetti, D. Neher, *J. Am. Chem. Soc.* **2014**, *136*, 4245.
[29] Z. Chen, P. Cai, J. Chen, X. Liu, L. Zhang, L. Lan, J. Peng, Y. Ma, Y. Cao, *Adv. Mater.* **2014**, *26*, 2586.
[30] a) P. W. Majewski, C. O. Osuji, *Langmuir* **2010**, *26*, 8737; b) G. Song, F. Kimura,T. Kimura , G. Piao, *Macromolecules* **2013**, *46*, 8957.
[31] R. Noriega, J. Rivnay, K. Vandewal, F. P. V. Koch, N. Stingelin, P. Smith, M. F. Toney, A. Salleo, *Nat. Mater.* **2013**, *12*, 1038.
[32] E. J. Meijer, G. H. Gelinck, E. V. Veenendaal, B. H. Huisman, D. M. de Leeuw, T. M. Klapwijk, *Appl. Phys. Lett.* **2003**, *82*, 4576.